Removal of reactive blue 19 from aqueous solution using rice straw fly ash

A.A. El-Bindary[1*], M.A. Abd El-Kawi[2], A.M. Hafez[2], I.G.A. Rashed[3], E.E. Aboelnaga[3]

[1]Departmentof Chemistry, Faculty of Science, University of Damietta, Damietta 34517, Egypt

[2]Department of Environmental Studies, Institute of Graduate Studies and Research, Alexandria University

[3]Department of Engineering Chemistry, Higher Institute for Engineering and Technology, Damietta, Egypt

Abstract

The adsorption behavior of reactive blue 19 dye (RB19) from aqueous solution onto rice straw fly ash (RSFA) was investigated in order to identify the ability of this waste adsorbent to remove colored textile dyes from wastewater. The effect of different variables in the batch method as a function of solution pH, contact time, concentration of adsorbate, adsorbent dosage and temperature were investigated and optimal experimental conditions were ascertain. More than 85 % removal efficiency was obtained within 60 min. at adsorbent dose of 0.09 g for initial dye concentration of 30-100mg/L at pH 1. The Brunauer-Emmett-Teller (BET) surface area and Barrett-Joyner-Halenda (BJH) pore volume were calculated and found to be 67.4 $m^2g^{-1}$and 0.134 cm^3g^{-1}, respectively. The point of zero charge (pH_{PZC}) of ACRS was determined and found to be 7.The experimental equilibrium data were tested by the isotherm models namely, Langmuir and Freundlich adsorption and the isotherm constants were determined. The kinetic data obtained with different initial concentration and temperature were analyzed using a pseudo-first-order and pseudo-second-order equations. The activation energy of adsorption was also evaluated and found to be +18.87 $kJ.mol^{-1}$ indicating that the adsorption is physisorption. Thermodynamic parameters, such as Gibbs free energy, enthalpy and entropy of adsorption of the dye-rice straw fly ash systems were evaluated and it was found that the reaction was spontaneous and exothermic in nature.

Keywords: Adsorption; Rice straw fly ash; Reactive blue 19; Kinetics; Thermodynamics.

1. Introduction

Dyes are an important class of pollutants which came in large amounts from textile, dyeing, paper and pulp, tannery and paint industries [1]. Therefore, these industrial effluents must be treated before discharge. Currently, much attention has been paid to the removal of dyes from industrial wastewater [2]. Various treatment methods including physical, chemical and biological schemes have been developed to remove dyes from wastewater [3]. Some of the applied techniques for the treatment of dye contaminated wastewaters are flocculation, coagulation, precipitation, adsorption, membrane filtration, electrochemical techniques, ozonation and fungal decolorization [4-6].Among them, adsorption has been recognized as a promising technique due to its high efficiency, simplicity of design, ease of operation as well as the wide suitability for diverse types of dyes[7,8].Because the dye effluent may cause damage to aquatic biota and human by mutagenic and carcinogenic effects, the removal of dye pollutants from wastewater is of great importance [9].Therefore, many industries use adsorption technique for reducing hazardous organic/inorganic pollutants present in effluents [10,11].

The Egyptian Environmental Protection Agency regarded rice straw fly ash adsorption as the best available technology for the removal of organic contaminants limited in the environmental regulations. In Egypt, rice straw is an easily available agricultural waste material, produced in large quantities as a by-product of rice milling and create potential environmental problems. The waste products which are the main contributors to biomass burning are wheat residue and rice straw. The disposal of rice straw by open-field burning frequently causes serious air pollution, hence new economical technologies for rice straw disposal and utilization must be developed. In order to improve the sorption capacity of these biomaterials, the low cost agricultural by-products were converted to fly ash. Fly ash is enriched with SiO_2 and contains a portion of unburned carbon, this waste possess the potentiality of a low-cost adsorbent to remove various hazardous materials from wastewater [12].In continuation to our earlier work [13,14] we investigate the adsorption of reactive blue 19 dye onto rice straw fly ash as a waste adsorbent. The point of zero charge determination (pH_{PZC}) of RSFA was determined. Effects of different parameters such as initial adsorbate concentration, adsorbent dosage, contact time, solution pH and temperature were studied. The kinetic and thermodynamic parameters were also calculated to determine rate constants and adsorption mechanism. The experimental data were fitted into Langmuir and Freundlich equations to determine which isotherm gives the best correlation to experimental data.

2. Materials and methods

2.1. Physical measurements

FTIR spectrum of rice straw fly ash (KBr discs, 4000-400 cm^{-1}) by Jasco-4100 spectrophotometer was obtained. The SEM results of the RSFA sample before and after the adsorption processes were obtained using (JEOL-JSM-6510 LV) scanning microscope to observe surface modification. UV-visible spectrophotometer (Perkin-Elmer AA800 Model AAS) was employed for absorbance measurements of samples. An Orion 900S2 model digital pH meter and a Gallenkamp Orbital Incubator were used for pH adjustment and shaking, respectively. N_2 adsorption/desorption isotherms on RSFA at 77 K was measured on a Quantachrome Nova Instruments version 10, from which the Brunauer-Emmett-Teller (BET) surface area and Barrett-Joyner-Halenda (BJH) pore volume were calculated.

2.2. Reactive blue 19 dye

Reactive blue 19 dye used in this study was purchased from Sigma-Aldrich and used without further purification. The dye information was presented in **Table 1**. A stock solution of 1000 mg/L was prepared by dissolving accurately weighed amounts of RB19 in separate doses. The desirable experimental concentrations of solutions were prepared [15] by diluting the stock solution with bidistilled water when necessary.

2.3. Preparation of rice straw fly ash

Rice straw fly ash (RSFA) as adsorbent was collected from Tammy Amdid, Dakahlia, Egypt Biogas Factory [14]. The concept is based on the burning of waste rice straw in a special incinerator at the temperature of 1000-1200 ℃.During the burning process the hydrocarbons are converted to carbon oxides, hydrogen, methane, propane and other gases. The carbon waste was left to cool down. In our laboratory the fly ash made from rice straw (RSFA) was crushed, ground and sieved through a 170 μm sieve and washed several times with bidistilled water. The adsorbent sample was dried at 120℃ for 48 h. preserved in the desiccators over anhydrous $CaCl_2$ for further use.

2.4. Determination of point of zero charge

The point of zero charge (pH_{PZC}) was determined by solid addition method [16]. A series of 0.1 M KNO_3 solutions (50 ML each) were prepared and their pH values were adjusted in the range of 1.0 to 12.0 by addition of 0.1 mol/L HCl and 0.1 mol/L NaOH. To each solution, 0.1 g of RSFA was added and the suspensions were shaked manually and the solution was kept for a period of 48 h with intermittent manual shaking. The final pH

of the solution was recorded and the difference between initial and final pH (ΔpH) (Y-axis) was plotted against the initial pH (X-axis). The point of this curve yielded pH_{PZC}.

Table 1: Properties of the adsorbate (RB19) used in the study.

Parameter	Characteristic
Name	Reactive blue 19
Symbol	RB19
Type color	Anionic
Chemical formula	$C_{22}H_{16}N_2Na_2O_{11}S_3$
Molecular weight (g/mol)	626.54
Wavelength of maximum absorption (nm)	595
Molar extinction coefficient, ε_{595} ($M^{-1} cm^{-1}$) 10000	
Chemical structure of color	
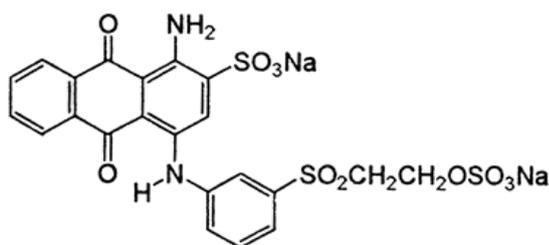
2.5. Adsorption experiments

Batch adsorption studies were carried out by shaking 100 ml conical flasks containing 0.09 g of (RSFA) and 25 mL of dye solutions of desired concentration with adjusted pH on an orbital shaker machine at 200 rpm at 25 °C. The solution pH was adjusted with 0.1 mol/L HCl and 0.1 mol/L NaOH solutions. At the end of the adsorption period, the supernatant solution was separated by centrifugation at 200 rpm for 10 min. Then the concentration of the residual dye was determined spectrophotometrically by monitoring the absorbance at 595 nm for dye using UV–Vis spectrophotometer. Percentage of Dye removal (R) was calculated using eq. (1):

$$R = 100 (C_o - C_t) / C_o \qquad (1)$$

where C_o (mg/L) and C_t (mg/L) are dye concentration initially and at time t, respectively. For adsorption isotherms, dye solutions different concentrations (30–100 mg/L) were agitated with known amounts of adsorbents until the equilibrium was achieved. Equilibrium adsorption capacity, q_e (mg dye per g adsorbent) was calculated from the following eq. (2):

$$q_e = V (C_o - C_t) / W \qquad (2)$$

where C_t (mg/L) is the dye concentration at equilibrium, V (L) is the volume of solution and W (g) is the weight of adsorbent.

The procedures of kinetic experiments were identical with those of equilibrium tests. At predetermined moments, aqueous samples (5 mL) were taken from the solution, the liquid was separated from the adsorbent and concentration of dye in solution was determined spectrophotometrically at a wavelength of 595 nm. The amount of dye adsorbed at time t, q_t (mg/g) was calculated by following eq. (3):

$$q_t = V (C_o - C_t) / m \qquad (3)$$

where C_o (mg/L) is the initial dye concentration, C_t (mg/L) the dye concentration at any time t, V (L) the volume of the solution and m (g) is the mass of the adsorbent.

In an adsorption study, it is necessary to fit the equilibrium adsorption data using different adsorption isotherm models and kinetic equations in order to analyze and design an adsorption process [13].

3. Results and discussion

3.1. Characterization of rice straw fly ash

Chemical composition of RSFA as determined by chemical analysis is C and O contents were C (40 %) and O (11 %) in the organic fraction of RSFA accounted for 51% of RSFA (wt. %). A small amounts of nitrogen (1.3 %), hydrogen (2.2 %) while the other metals were trace. The O content in RSFA was contributed by functional groups (e.g., hydroxyl and carbonyl) and C–O–C bonds. The Si content was (23 %) and present as silica in RSFA, since silica is a natural constituent in rice straw and remains after rice straw burning.

3.2. FTIR measurements

FTIR technique was used to examine the particular vibration of the surface groups and bonds responsible for dye adsorption. The major peaks on the surface of RSFA was observed at FTIR (KBr) (v cm^{-1}): 3397 (-SiOH or -OH); 1585 (C=O); 1195 (Si-O-Si) and 792 (Si-H) cm^{-1} [17].The adsorption bands of RB19 was observed at FTIR (KBr) (v cm^{-1}): 3400 (-OH of the hydroxide layer and interlayer water); 1346 and 1204 ($v_{as}(SO_2)$ and $v_s(SO_2)$, respectively); region 1620-1404 (C=C aromatic ring);1640, 1300 and 1188 (C=O, C-O and C-N, respectively) [18].By comparing the spectrum of RSFA and RSFA-RB19, the stretching adsorption bands of O-H and Si-O of RSFA were diminished and shifted to higher frequencies, respectively as a function of chemical interaction of RB19 with RSFA. Furthermore, the bands assigned to aromatic skeletal vibrations of RB19 have been shifted, broadened and reduced after adsorption on RSFA. All these findings suggest the attachment of RB19 on the RSFA [19].

3.3. Brunauer-Emmett-Teller (BET) surface area

The Brunauer-Emmett-Teller (BET) [20] surface area and Barrett-Joyner-Halenda (BJH) pore size of RSFA have been investigated using N_2 adsorption/desorption measurements at 77 K (**Fig. 1**).
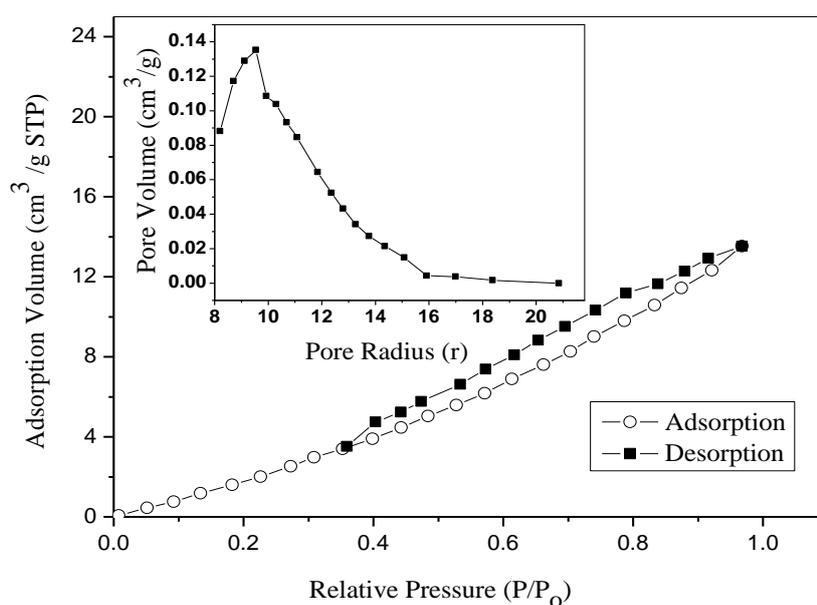
Fig. 1: BET adsorption-desorption isotherms and pore volume distribution (insert) of RSFA [7].

The BET surface area of RSFA was obtained as 67.4 m^2 g^{-1} can supply more surface active sites, leading to an enhancement of adsorption performance [7]. It is suggested that the pore structure of the adsorbent RSFA consists of macropores, mesopores and micropores. The total pore volume (V$_p$) at P/P$_o$ = 0.959 was obtained as 0.134 cm^{3}g^{-1}, which indicating that RSFA has a mesoporous structure and makes it easy for RB19dye to penetrate into the mesopores of RSFA.

3.4. Determination of point of zero charge (pH$_{PZC}$)

The pH$_{PZC}$ gives very significant information about the type of surface active centres. The pH$_{PZC}$ of RSFA was found to be 7. This shows that below this pH, the RSFA acquires a positive charge due to protonation of functional groups and above this pH, negative charge exists on the surface of RSFA. The adsorption of anionic dyes is favoured at pH < pH$_{PZC}$ where the surface becomes positively charged [21].

3.5. SEM analysis

Scanning electron microscopy (SEM) has been a primary tool for characterizing the surface morphology and fundamental physical properties of the adsorbent surface. It is useful for determining the particle shape, porosity and appropriate size distribution of the adsorbent. Scanning electron micrographs of raw RSFA and adsorbed RB19 onto RSFA are shown in **Figs. 2** and **3**, respectively. As illustrated from **Fig. 2**, the RSFA mainly constituted of hollowed spheres of different size and some unshaped fragments ascribed to unburned rice straw. It might also be seen in the micrograph where some of the smaller size particles were adhered on bigger size particles. **Fig. 3**, illustrated very distinguished dark spots which can be taken as a sign of effective adsorption of RB19 molecules in the cavities and pores of this adsorbent.
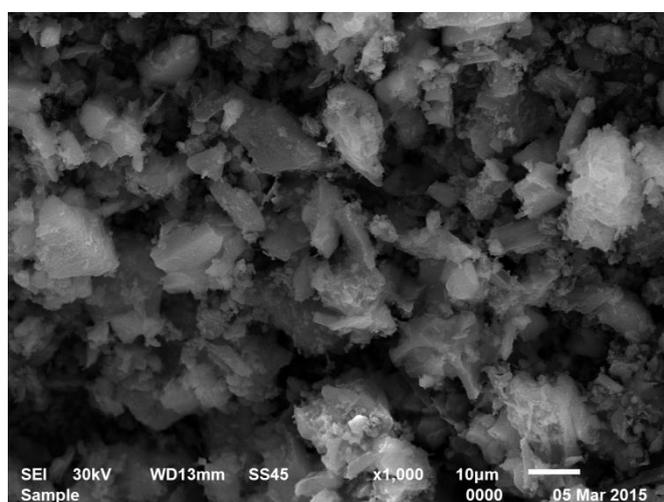
Fig. 2: SEM of RSFA before adsorption of RB19 dye.   **Fig. 3:** SEM of RSFA after adsorption of RB19 dye.
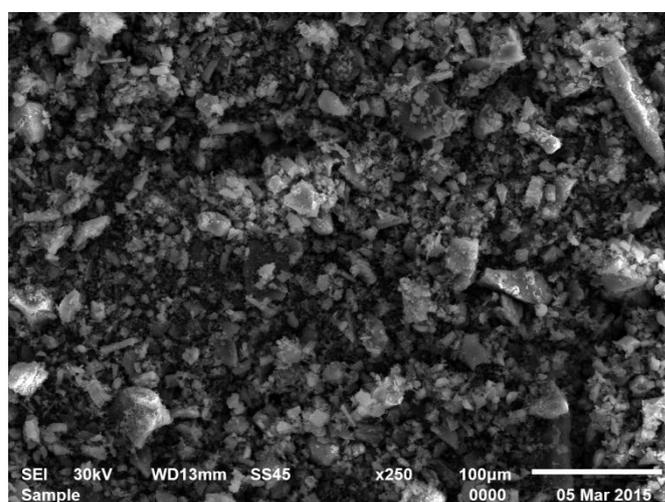
3.6. Effect of pH

One of the most important parameters that affect the adsorption of dye molecules is pH of solution. The removal of RB19 dye by RSFA at different pH values was studied at initial concentrations of 100 mg/L of the dye, 25 °C and 0.09 g/L adsorbent dosage. RSFA has proved to be an effective adsorbent for the removal of the dye, which was achieved via adsorption from an aqueous solution at pH 1 was achieved (**Fig. 4**). It shows that the adsorption capacity of tested dye onto RSFA increases significantly with decreasing pH. The maximum removals for contact time 60 min. were carried out at pH 1. In acidic solutions, the surface of RSFA has positive charge due to the increase in the H$^+$ ions in the solution, which leads to strong electrostatic adsorption between the positive charge of the carbon surface and anions of the dye molecule and increase the adsorption rate. In high pH levels, hydroxyl ions compete with the dye anions for the adsorption sites [20,22].
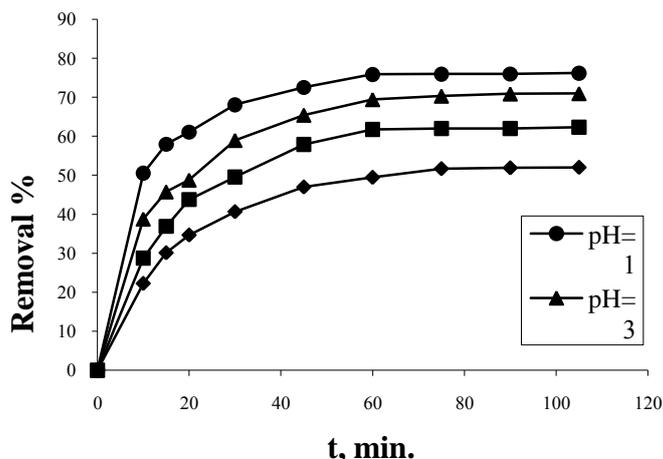
Fig. 4. Effect of pH on adsorption of RB19 dye
onto RSFA at dosage 0.09 g/l, pH=1 and
temperature 25 °C.

3.7. Effect of dye concentrations

The removal of RB19 dye by adsorption on the adsorbent (RSFA)was shown to increase with time and attained a maximum value at about 60 min, and thereafter, it remained almost constant (**Fig. 5**). On changing the initial concentration of dye solution from 30 to 100 mg/L at 25 °C, pH 1 and 0.09 g/L adsorbent dosage the amount of removed dyes was decreased. It was clear that the removal of the dye was dependent on the initial concentration of the dye because the decrease in the initial dye concentration increased the amount of dye adsorbed. This is very clear because, for a fixed adsorbent dose, the number of active adsorption sites to accommodate adsorbate ions remains unchanged but with increasing adsorbate concentration, the adsorbate ions to be accommodated increase and hence the percentage of adsorption goes down.
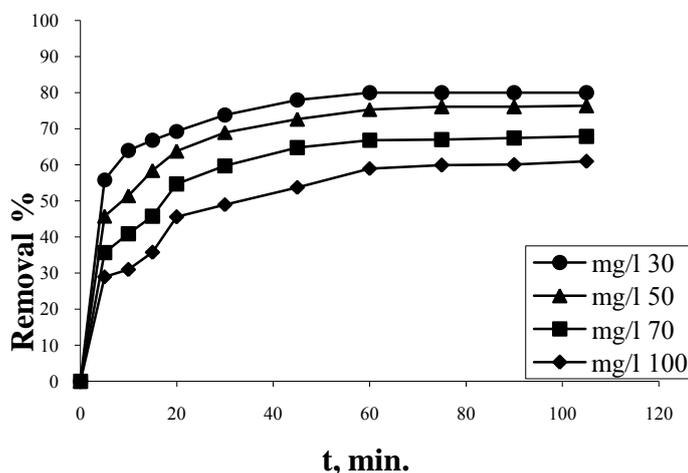
Fig. 5. Effect of intial dye concentration on
adsorption of RB19 dye onto RSFA, dosge 0.09
g/l, pH 1 and 25 °C.

3.8. Effect of adsorbent dosage

The adsorbent dose is an important parameter in adsorption studies because it determines the capacity of adsorbent for a given initial concentration of dye solution. The uptake of RB19 dye with change in adsorbent dosage (0.01–0.09 g) at adsorbate concentrations of 100 mg/L at 25 °C and pH 1 is presented at (**Fig. 6**) Adsorption of dye shows that the uptake of dye per gram of adsorbent increases with increasing adsorbent dosage from 0.01 to 0.09 g. This is because a higher dose of adsorbent, led to increased surface area and more adsorption sites are available causing higher removal of the dye. Increasing the RSFA dose increases the

probability of the RSFA entanglement in the solution, causing adsorption in the interlayer space and a decrease in the aggregation of RB19 at the external surface. Accordingly, the adsorption capacity declined as the RSFA dosage increased. Moreover, the high RSFA dosage may influence the physical characteristics of the solid-liquid suspensions, such as by increasing the viscosity and inhibiting the diffusion of RB19 molecules to the surface of RSFA.
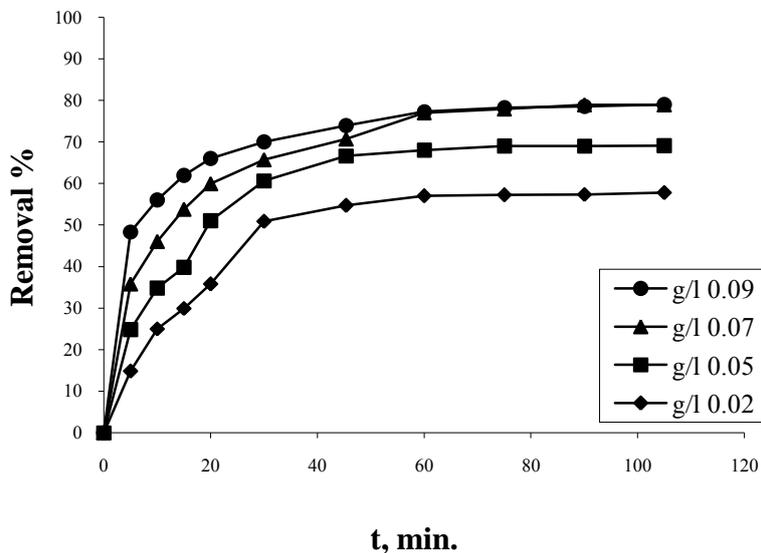
Fig. 6. Effect of dosage on the adsorption of RB19 dye at concentration 100 mg/l, pH=1 and 25 ºC.

3.9. Effect of temperature

Temperature is an important parameter in the adsorption process (**Fig. 7**) which explain the relation between the removal of dye ratio and time at different temperatures (25, 40, 50 and 60ºC) onto RSFA.
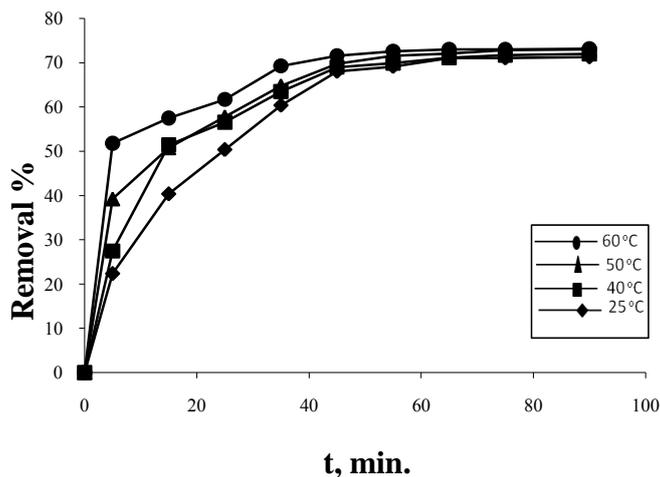
Fig. 7. Effect of temperature on adsorption of RB19 dye onto RSFA, dosage 0.09 g/l, pH=1 and temperature 25 ºC.

In our case the experimental data obtained at pH 1, adsorbent dosage 0.09 g/L, and initial concentration of 100 mg/L show that increase in the adsorption capacity at temperatures from 25 to 60 ºC. This may be attributed to the fact that at high temperature, the mobility and diffusion rate of dye molecules increased, while the solution

viscosity decreased, which is due to the existence of available empty surfaces during the early stages of adsorption.

3.10. Equilibrium isotherms

Equilibrium data, generally known as adsorption isotherms, are important in the basic design of adsorption systems, and are critical in optimizing the use of adsorbents. To optimize the design of an adsorption system for removing RB19 from solutions, it is essential to establish the most appropriate correlation for the equilibrium curves [24-26]. Several isotherms equations are available and two important isotherms are applied to fit the equilibrium data in this study; Langmuir and Freundlich isotherms are listed in **Table 2**.

Langmuir adsorption isotherm assumes monolayer adsorption of adsorbate over a homogeneous adsorbent surface with finite number of identical sites, which are energetically equivalent and negligible interaction between the adsorbed molecules. Theoretically, the sorbent has a finite capacity for the sorbate. Therefore, a saturation value is reached beyond which no further sorption can occur. The Langmuir adsorption isotherm in the linear form is expressed as the following equation [27-31],

$$C_e / q_e = 1/ (q_{max}K_L) + C_e / q_{max} \qquad (4)$$

where C_e is the equilibrium dye concentration (mg/L), q_e is the equilibrium amount of adsorbed dye per unit weight of adsorbent (mg/g), q_{max} is the maximum amount of adsorbed dye per unit weight of adsorbent to form a complete monolayer coverage (mg/g) and K_L is the Langmuir adsorption constant (L/mg).Therefore, a plot of C_e/q_e vs. C_e (**Fig. 8**), gives a straight line of slope $1/q_{max}$ and the intercept $1/(q_{max}K_L)$. The Langmuir equation is applicable to homogeneous sorption, where the sorption of each sorbate molecule onto the surface is equal to the sorption activation energy.

The Freundlich adsorption isotherm assumes multilayer adsorption and it is applicable to adsorption on heterogeneous surfaces with interaction between the adsorbed molecules. The Freundlich isotherm [30-32] is expressed as the following equation:

$$q_e = K_F . C_e^{1/n} \qquad (5)$$

where q_e is the equilibrium dye concentration on adsorbent (mg/g), C_e is the equilibrium dye concentration in solution (mg/L), K_F is the Freundlich adsorption constant (L/g) and $1/n$ is the heterogeneity factor. A linear form of the Freundlich expression can be obtained by taking logarithms of the equation

$$log q_e = log K_F + 1/n . log C_e \qquad (6)$$

Therefore, a plot of log q_e *vs.* log C_e for the adsorption of tested dye onto RSFA (**Fig. 9**) was employed to generate the intercept value of K_F and the slope of $1/n$.

The model parameters and correlation coefficients for Langmuir (r_L^2) and for Freundlich (r_F^2) values are compared in **Table 2**. From the values of the correlation coefficient in Table 2, it is clear that the adsorption curves fit better to the Freundlich isotherm than Langmuir isotherm, indicating that the adsorption of RB19 onto RSFA adsorbent is multilayer coverage. Furthermore, the surface of (RSFA) is mostly made up of heterogeneous adsorption batches. The highest value of n at equilibrium is 1.81 (**Table 2**), which would seem to suggest that the adsorption is physical, which is referred the adsorption bond which becomes weak [33,34] and conducted with Van der Waals forces.

Table 2: Langmuir and Freundlich parameters for the adsorption of RB19 dye onto RSFA.

Temperature (°C)	Langmuir isotherm			Freundlich isotherm		
	q_{max} (mg/g)	K_L (L/gm)	r_L^2	K_F (mg/g)	n	r_F^2
25	38.24	0.2199	0.997	0.927	1.178	0.998
40	105.69	0.0620	0.993	0.951	1.181	0.995
50	208.19	0.0329	0.995	0.950	1.180	0.996
60	221.12	0.0320	0.994	0.864	1.164	0.999
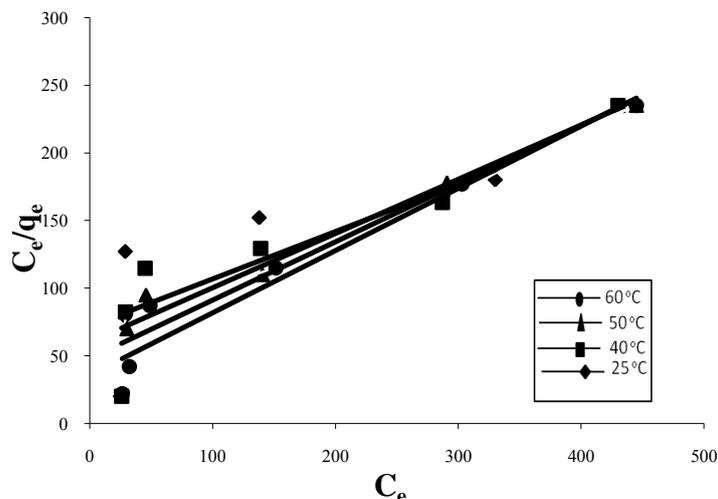
Fig. 8. Langmuir plot for the adsorption of
RB19 dye onto RSFA at different
temperatures.
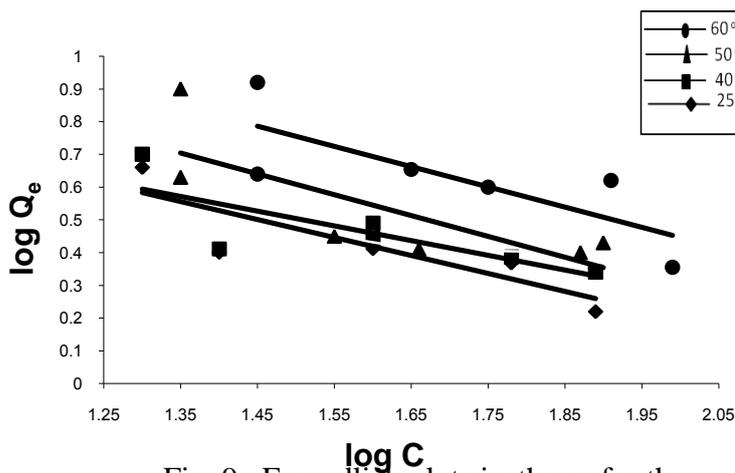
Fig. 9. Freundlich plots isotherm for the
adsorption of RB19 dye onto RSFA at different
temperatures.

3.11. Adsorption kinetics

Kinetic models not only allows estimation of adsorption rates but also leads to suitable rate expressions characteristic of possible reaction mechanisms. In this respect, two kinetic models including the pseudo-first-order and pseudo-second-order equations were investigated to fit the experimental data [35,36]. The rate of removal of RB19 by adsorption was rapid initially and then slowed gradually until it attained an equilibrium beyond which there was a significant increase in the rate of removal. The maximum adsorption was observed at 60 min. and it is thus fixed as the equilibrium time.

The pseudo-first-order rate expression of Lagergren [35,36] is given as:

$$\log (q_e - q_t) = \log q_e - k_1 t \qquad (7)$$

The pseudo-second-order kinetic model [36] is expressed as:

$$t/q_t = 1/k_2 q_2^2 + 1/q_2\, t \qquad (8)$$

where qt is the amount of dye adsorbed (mg/g) at various times t, q_e is the maximum adsorption capacity (mg/g) for pseudo-first-order adsorption, k_1 is the pseudo-first-order rate constant for the adsorption process (min^{-1}), q_2 is the maximum adsorption capacity (mg/g) for the pseudo-second-order adsorption, k_2 is the rate constant of

pseudo-second-order adsorption (g mg^{-1} min^{-1}). The straight-line plots of log $(q_e - qt)$ versus t for the pseudo-first-order reaction and t/qt vs. t for the pseudo-second-order reaction (**Figs.10** and **11**) for the adsorption of RB19 onto RSFA have also been tested to obtain the rate parameters. The k_1, k_2, q_e, q_2, and correlation coefficients, r_1^2 and r_2^2 for the dye under different temperatures were calculated from these plots and are given in **Table 3.** As shown, the kinetics of RB19 removal by RSFA followed the pseudo-second-order kinetic equation with correlation coefficients $(r_2^2) > 0.998$.

Table 3: Pseudo-first-order and Pseudo-second-order for the adsorption of RB19dye onto RSFA.

Temperature	Pseudo-first-order			Pseudo-second-order		
	q_e	k_1	r_1^2	q_2	k_2	r_2^2
(^{o}C)	(mg/g)	(min^{-1})		(mg/g)	(g mg^{-1} min^{-1})	
25	0.951	4.181	0.996	149.33	0.192	0.999
40	0.926	4.141	0.981	145.98	0.371	0.999
50	0.951	3.215	0.868	145.19	0.569	0.998
60	0.945	3.240	0.986	144.33	0.647	0.999
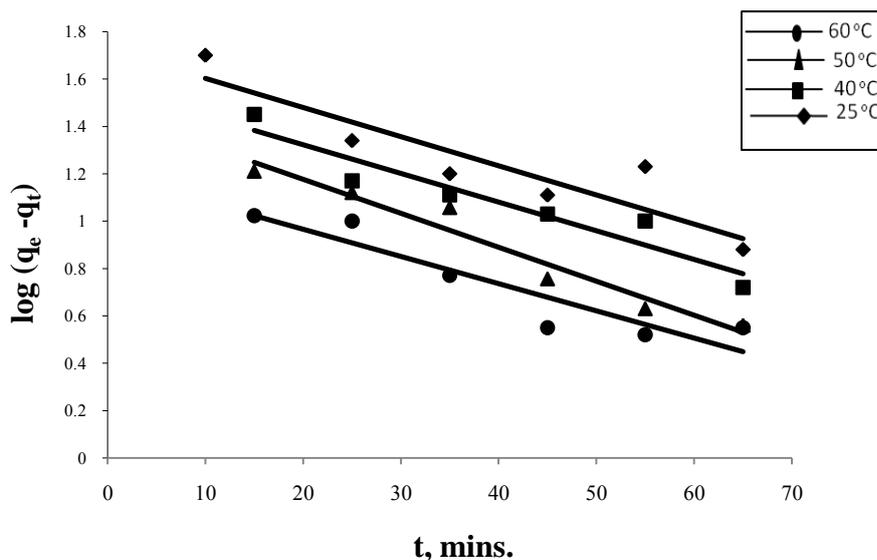
Fig. 10. Pseudo-first-order kinetic plot for the
adsorption at different temperatures.

3.12. Thermodynamic parameters

In any adsorption process, both energy and entropy considerations must be taken into account in order to determine what process will occur spontaneously. Values of thermodynamic parameters are the actual indicators for practical application of a process. The amount of RB19 adsorbed onto RSFA at equilibrium and at different temperatures 25, 40, 50 and 60 ^{o}C, has been examined to obtain thermodynamic parameters for the adsorption system. The pseudo-second-order rate constant of tested dye adsorption is expressed as a function of temperature by the following Arrhenius type relationship [37]:

$$\ln k_2 = \ln A - E_a/RT \qquad (9)$$

where E_a is the Arrhenius activation energy of adsorption, A is the Arrhenius factor, R is the gas constant and is equal to 8.314 J.mol^{-1} K^{-1} and T is the operated temperature.
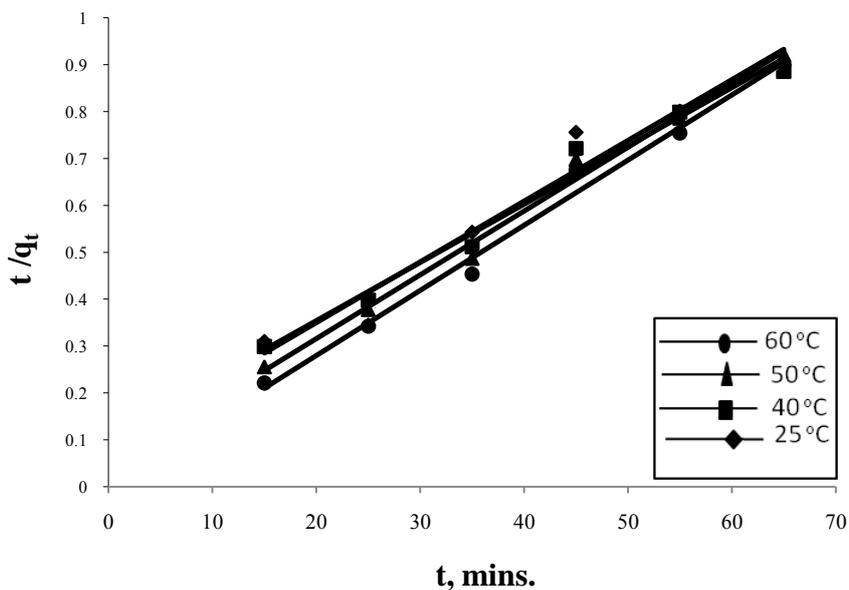
Fig. 11. Pseudo-second-order kinetic plot for the adsorption at

different temperatures.

A linear plot of ln k_2 *vs.* 1/T for the adsorption (**Fig. 12**) was constructed to generate the activation energy from the slope ($-E_a/R$). The chemical (chemisorption) or physical (physisorption) adsorption mechanism are often an important indicator to describe the type of interactions between RB19 and RSFA. The magnitude of activation energy gives an idea about the type of adsorption which is mainly physical or chemical. Low activation energies (5–40 kJ/mol) are characteristics for physisorption, while higher activation energies (40–800 kJ/mol) suggest chemisorption [38]. The result obtained is +18.87kJ/mol (**Table 4**) for the adsorption of RB19 onto RSFA, indicating that the adsorption has a low potential barrier and corresponding to a physisorption.
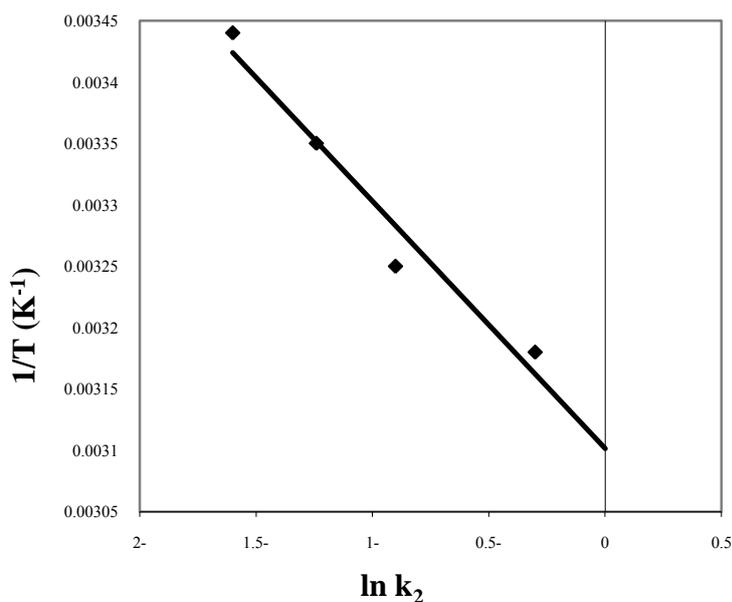
Fig. 12. Arrhenius plot of the adsorption of RB19
dye onto RSFA.

The other thermodynamic parameters, change in the standard free energy (ΔG^o), enthalpy (ΔH^o) and entropy (ΔS^o) were determined by using following equations:

$$K_C = C_A/C_S \qquad (10)$$
$$\Delta G^o = -RT \ln K_C \qquad (11)$$
$$\ln K_C = \Delta S^o/R - \Delta H^o/RT \qquad (12)$$

where K_C is the equilibrium constant, C_A is the amount of RB19 adsorbed on RSFA of the solution at equilibrium (mg/L), and C_S is the equilibrium concentration of the dye in the solution (mg/L). The q_2 of the pseudo-second-order model in Table 3 was used to obtain C_A and C_S. T is the solution temperature (K) and R is the gas constant. ΔH^o and ΔS^o were calculated from the slope and the intercept of Van't Hoff plots of $\ln K_C$ *vs.* 1/T (**Fig. 13**). The results are given in **Table 4**.

The values of adsorption thermodynamic parameters are listed in Table 4. The negative value of the change of free energy (ΔG^o) confirms the feasibility of the adsorption process and also indicates spontaneous adsorption of RB19 onto RSFA in the temperature range studied [39]. The small negative value of the standard enthalpy change (ΔH^o) which is (-19.58 kJ/mol) indicates that the adsorption is physical in nature involving weak forces of attraction and is also exothermic, thereby demonstrating that the process is stable energetically [40-42].

Table 4: Thermodynamic parameters calculated with the pseudo-second rate constant for RB19 dye onto RSFA.

Temperature (^{o}C)	K_c	Ea (kJ mol^{-1})	ΔG^o (kJ mol^{-1})	ΔH^o (kJ mol^{-1})	ΔS^o (J.mol^{-1}.K^{-1})
25	87.44		-30.35		
40	147.34	18.87	-30.57	-19.58	0.039
50	222.21		-30.89		
60	202.95		-31.23		

Fig. 13. Van't Hoff plot for determination of thermodynamic parametets for the adsorption.
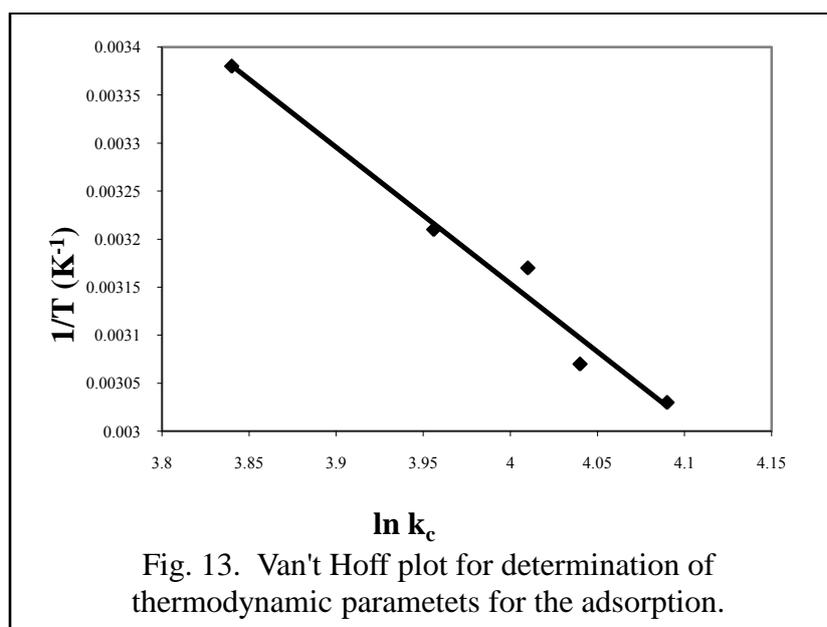
Conclusion

From the present study which clearly demonstrated that rice straw fly ash (RSFA) are an effective adsorbent for the removal of RB19 from an aqueous solution and polluted water. The high adsorption capacity of RB19 onto RSFA in highly acidic solutions (pH 1) is due to the strong electrostatic interactions between its adsorption site

and dye anion. The Brunauer-Emmett-Teller (BET) surface area and Barrett-Joyner-Halenda (BJH) pore volume were calculated and found to be 67.4 m^2 g^{-1} and 0.134 cm^3 g^{-1}, respectively. The point of zero charge (pH_{PZC}) of RSFA was determined and found to be 7. SEM images shows well defined and characterized morphological images that are evident for the effective adsorption of RB19 molecules on the cavities and pores of RSFA. For the application of Langmuir and Freundlich equations, the experimental results show that the Freundlich model was the best. The highest value of n at equilibrium is 1.181 suggest that the adsorption is physical. The kinetic data tends to fit very well in the pseudo-second-order kinetics model with high correlation coefficients. The ΔG^o values were negative, therefore the adsorption was spontaneous in nature. The negative value of ΔH^o reveals that the adsorption process was exothermic in nature and a physical adsorption. The positive value of ΔS^o implies that the increment of an orderliness between the adsorbate and the adsorbent molecules. Finally, the adsorbent RSFA displayed the main advantages of excellent dispersion in an aqueous solution, separation convenience and high adsorption capacity, which implied their application potentials for effective removal of other dye pollutants from an aqueous solution.

References

1. Anastopoulos I., Kyzas G.Z., *J. Mol. Liq.* 200 (2014) 381-389.
2. Fu J., Chen Z., Wang M., Liu S., Zhang J., Zhang J., Han R., Xu Q., *Chem. Eng. J.* 259 (2015) 53-61.
3. Ma T.T., Chang P.R., Zheng P.W., Zhao F., Ma X.F., *Chem. Eng. J.* 240 (2014) 595–600.
4. Mahjoub B., Ben Brahim I., *J. Mater. Environ. Sci.* 6 (11) (2015) 3359-3370.
5. El-Bindary A.A., Hussien M.A., Diab M.A., Eessa A.M., *J. Mol. Liq.* 197 (2014) 236-242.
6. El-Bindary A.A., Diab M.A., Hussien M.A., El-Sonbati A.Z., Eessa A.M., *Spectrochim. Acta A* 124 (2014) 70-77.
7. El-Bindary A.A., El-Sonbati A.Z., Al-Sarawy A.A., Mohamed K.S., Farid M.A., *J. Mol. Liq.* 199 (2014) 71-78.
8. Aarfane A., Tahiri S., Salhi A., El Kadiri Boutchich G., Siniti M., Bensitel M., Sabour B., El Krati M., *J. Mater. Environ. Sci.* 6 (10) (2015) 2944-2957.
9. Cheng Z., Zhang L., Guo X., Jiang X., Li T., *Spectrochim. Acta A* 137 (2015) 1126-1143.
10. Gupta V.K., Jain R., Nayak A., Agarwal S., Shrivastava M., *Mater. Sci. Eng. C* 31 (2011) 1062-1067.
11. Guzel F., Saygili H., Saygili G.A., Koyuncu F., *J. Mol. Liquids* 194 (2014) 130-140.
12. Sun D., Zhang X., Wu Y., Liu X., *J. Hazard. Mater.* 181 (2010) 335-342.
13. El-Bindary A.A., El-Sonbati A.Z., Al-Sarawy A.A., Mohamed K.S., Farid M.A., *J. Mater. Environ. Sci.* 6 (2015) 1-10.
14. El-Bindary A.A., El-Sonbati A.Z., Al-Sarawy A.A., Mohamed K.S., Farid M.A., *Spectrochim. Acta A* 136 (2015) 1842-1849.
15. Salvachúa D., Prieto A., Martínez Á.T., Martínez M.J., *Appl. Env. Microbiol.* 79 (2013) 4316-4324.
16. Daffalla S.B., Mukhtar H., Shaharun M.S., *J. Appl. Sci.* 10 (2010) 1060-1067.
17. Mall I.D., Shrivastava V.C., Kumar G.V.A., Mishra I.M., *Colloids Surf. A: Physicochem. Eng. Aspects* 278 (2006) 175-187.
18. Elkhattabi E., Lakraimi M., Badreddine M., legrouri A., Cherkaoui O., Berraho M., *Appl. Water Sci.* 33 (2013) 431-438.
19. Dizge N., Aydiner C., Demirbas E., Kobya M., Kara S., *J. Hazard. Meter.* 150 (2008) 737-746.
20. S. Brunauer S., Emmett P.H., Teller E., *J. Am. Chem. Soc.* 60 (2002) 309-319.
21. Sadaf S., Bhatti H.N., Arif M., Amin M., Nazar F., *Chem. Ecol.* 31 (2015) 252-264.
22. Alkan M., Demirbas O., Celikcapa S., Dogan M., *J. Hazard. Mater.* 116 (2004) 135-145.
23. Khan M.R., Ray M., Guha A.K., *Bioresour. Technol.* 102 (2011) 2394-2399.
24. Guendy H.R., *J. Appl. Sci. Res.* 6 (2010) 964-972.
25. Kiran I., Akar T., Ozcan A.S., Ozcan A., Tunali S., *Biochem. Eng. J.* 31 (2006) 197–203.

26. Yavuz M., Gode F., Pehlivan E., Ozmert S., Sharma Y.C., *Chem. Eng. J.* 137 (2008) 453-461.
27.   Langmuir I., *J. Am. Chem. Soc.* 38 (1916) 31-60.
28.   Langmuir I., *J. Am. Chem. Soc.* 39 (1917) 1848-1906.
29.   Langmuir I., *J. Am. Chem. Soc.* 40 (1918) 1361-1403.
30. Alley A.R., "Water quality control handbook", *McGraw-Hill Education*: Europe: London; (2000) pp.125-141.
31. Woodard F., "Industrial waste treatment handbook", *Butterworth-Heinemann*: Boston (2001) pp. 376-451.
32. Freundlich H.M.F., *Z. Phys. Chem. (Leipzig)* 57A (1906) 385-470.
33. Tunali S., Ozcan A.S., Ozcan A., Gedikbey T., *J. Hazard. Mater.* B 135 (2006) 141-148.
34. Jiang J.-O., Cooper C., Ouki S., *Chemosphere* 47 (2002) 711-716.
35. Lagergren S., *Handlingar* 24 (1898) 1-39.
36. Ho Y.S., McKay G., *Chem. Eng. J.* 70 (1998) 115-124.
37. Juang R.S., Wu F.C., Tseng R.L., *Environ. Technol.* 18 (1997) 525-531.
38. Nollet H., Roels M., Lutgen P., Van der Meeren P., Verstraete W., *Chemosphere* 53 (2003) 655-665.
39. Jaycock M.J., Parfitt G.D., "Chemistry of Interfaces", Ellis Horwood Ltd, Onichester, 1981.
40. Elwakeel K.Z., El-Bindary A.A., El-Sonbati A.Z., Hawas A.R., RSC Adv. 6(4) (2016) 3350-3361.
41. Ghaedi M., Nasiri K.S., *Spectrochim. Acta A* 136 (2015) 141-148.
42. Amrhar O., Nassali H., Elyoubi M. S., *J. Mater. Environ. Sci.* 6 (11) (2015) 3054-3065.

(2016) ; http://www.jmaterenvironsci.com